Available online at www.sciencedirect.com
SCIENCE DIRECT®

Polymer Degradation and Stability 91 (2006) 21–30

Polymer Degradation and Stability

www.elsevier.com/locate/polydegstab

# Thermal degradation behaviour of aromatic poly(ester-amide) with pendant phosphorus groups investigated by pyrolysis-GC/MS

Wenjeng Guo [a], Wen-Tsuen Leu [b], Sheng-Huei Hsiao [b,*], Guey-Sheng Liou [c]

[a] Department of Chemical Engineering, National Taipei University of Technology, 1 Chunghsiao East Road, 3rd Section, Taipei 100, Taiwan, Republic of China
[b] Department of Chemical Engineering, Tatung University, 40 Chungshan North Road, 3rd Section, Taipei 104, Taiwan, Republic of China
[c] Department of Applied Chemistry, National Chi Nan University, 1 University Road, Nantou Hsien 545, Taiwan, Republic of China

Received 31 March 2005; accepted 28 April 2005
Available online 21 June 2005

## Abstract

The thermal stability of a novel phosphorus-containing aromatic poly(ester-amide) ODOP-PEA was investigated by thermogravimetric analysis (TGA). The weight of ODOP-PEA fell slightly at the temperature range of 300–400 °C in the TGA analysis, and the major weight loss occurred at 500 °C. The structural identification of the volatile products resulted from the ODOP-PEA pyrolysis at different temperatures was performed by pyrolysis-gas chromatography/mass spectrometry (pyrolysis-GC/MS). The P–C bond linked between the pendant DOPO group and the polymer chain disconnected first at approximately 275 °C, indicating that it is the weakest bond in the ODOP-PEA. The P–O bond in the pendant DOPO group was stable up to 300 °C. The cleavage of the ester linkage within the polymer main chain initiated at 400 °C, and the amide bond scission occurred at greater than 400 °C. The structures of the decomposition products were used to propose the degradation processes happening during the pyrolysis of the polymer.

*Keywords:* Poly(ester-amide); Thermal degradation; TGA; Pyrolysis-GC/MS

## 1. Introduction

Wholly aromatic polyamides (aramids) have been categorized as high-performance polymeric materials with several useful properties such as outstanding thermal stability, low flammability, good chemical resistance, and excellent mechanical properties [1–3]. However, aramids are usually difficult to process into useful forms due to their high glass-transition ($T_g$) or melting temperatures and limited solubility in common organic solvents; therefore, a great deal of effort has been made to improve the physical characteristics of the relatively intractable polymers. Those efforts include the introduction of flexible links [4–6], asymmetric units [7], bulky pendant groups [8–11], and kinked or non-coplanar structures [12–15] into the polymer chain.

---

* Corresponding author.
*E-mail address:* shhsiao@ttu.edu.tw (S.-H. Hsiao).

0141-3910/$ - see front matter © 2005 Elsevier Ltd. All rights reserved.
doi:10.1016/j.polymdegradstab.2005.04.026

These modifications have lowered the melting temperature and increased the solubility by reduction in crystallinity. Previously, we reported that the incorporation of both ester and naphthyl units into the polymer backbones may enhance the solubility and processability of aromatic polyamides without significant impairment of the thermal and mechanical properties [16]. Wang and coworkers [17–25] reported several phosphorus-containing polymer systems based on 2-(6-oxido-6*H*-dibenz[*c*,*e*][1,2]oxaphosphorin-6-yl)hydroquinone (ODOPHQ), a phosphorus (P)-diol derived from the addition reaction of 9,10-dihydro-9-oxa-10-phosphaphenanthrene 10-oxide (DOPO) with *p*-benzoquinone. Since the fire-retardant nature of P-containing materials is well known, the introduction of laterally attached DOPO groups has been shown to enhance the solubility and confer fire retardancy upon the polyamides.

Our group has always interested in preparing easily processable high-performance polymers bearing naphthyl units; we employ a strategy similar to that reported by Wang and Lin [20] for preparation of P-containing diesteramines, and a series of poly(ester-amide)s obtained with high aromatic contents, flexible ester segments, and bulky pendant phosphorus groups had been prepared [26]. All of those DOPO-containing poly(ester-amide)s prepared by our group showed enhanced flame retardancy and were soluble in various organic solvents with insignificant weight loss up to 440 °C in nitrogen. Further improving flame retardant properties and organosolubility of the DOPO-containing poly(ester-amide)s, Liu [27] employed aromatic diamine possessing two pendant DOPO groups to prepare polyamides, but these polymers exhibited low initial decomposition at 310–362 °C. Liu concluded that the pendant DOPO group detached from the polymer units at the initial decomposition temperature. Understanding of the thermal decomposition characteristic of a polymer is of crucial importance for practical application, and thermal degradation mechanisms of DOPO-containing polymers are still unclear due to the lack of direct experimental evidence from pyrolysis-GC/MS. The technique of pyrolysis has been employed for the identification of materials, analysis of compound structures, and helped understanding of poisonous pyrolysates. There are many studies of pyrolysis in the literatures by using TGA/FTIR [28], TGA/EGA/FTIR [29], TGA/GC/MS [30], and pyrolysis-GC/MS [31,32]. Recently, pyrolysis-GC/MS analysis has become the main approach in the thermal analysis of polymeric materials. In this work, we characterized the thermal degradation of the aromatic poly(ester-amide) (ODOP-PEA) with pendant phosphorus groups, and the structural identification of the volatile products resulted from the ODOP-PEA pyrolysis at different temperatures was made by pyrolysis-GC/MS.

## 2. Experimental

### 2.1. Materials

According to a modification of the method reported by Endo et al. [33] and Wang and Lin [21], 2-(6-oxido-6*H*-dibenz[*c*,*e*][1,2]oxaphosphorin-6-yl)-1,4-naphthalenediol (ODOP-N) was synthesized from the addition reaction of DOPO with 1,4-naphthoquinone. The phosphorus (P)-containing diesteramine **2** was prepared by hydrogen Pd/C-catalysed reduction of the dinitro compound **1** resulting from the condensation reaction of ODOP-N with 4-nitrobenzoyl chloride. The synthetic details and characterization data of the P-diesteramine **2** have been described in our previous publication [34]. The ODOP-PEA was synthesized from the P-diesteramine **2** with terephthaloyl chloride by low-temperature solution polycondensation in DMAc solution using propylene oxide (PPO) as an acid acceptor, as shown in Scheme 1. As reported in a previous article [26], the obtained ODOP-PEA exhibited a very high inherent viscosity of 3.2 dL/g and could be solution-cast into a very tough and strong thin film. The polymer is amorphous with a $T_g$ of about 267 °C, and it is stable to above 400 °C. It also showed high flame retardancy with a limiting oxygen index (LOI) of about 44.

### 2.2. Measurements

Thermogravimetric analysis (TGA) was conducted with a Perkin Elmer Pyris 1 TGA. Experiments were carried out on approximately 5 mg samples heated in flowing nitrogen (40 $cm^3$/min) at a heating rate of 20 °C/min from 200 to 800 °C. Pyrolysis-GC/MS analyses were run in a Frontier Laboratories model PY-2020iD Double-Shot Pyrolyser coupled to a Hewlett Packard 6890 series Gas Chromatograph linking to a Hewlett Packard 5973 Mass Selective Detector. The pyrolysis temperatures were respectively set at 300, 350, 400, 450, 500, 550, 600, and 700 °C. The pyrolysis gases from the ODOP-PEA were introduced directly into the GC/MS analysis system. The pyrolyser is based on a technique in which a small deactivated stainless steel cup loaded with a sample is dropped into a small sized vertical furnace by gravitational free-fall with push button mechanism. This system is designed to provide precise temperature control and minimal condensation of pyrolysates in the system. A sample of 1 mg ODOP-PEA was placed in the small stainless steel cup and attached it to the pyrolyser. After the GC conditions were established and the pyrolysis furnace heated up to 300 °C at a heating rate of 20 °C/min, the sample cup was dropped into the pyrolysis furnace by manually pressing the sample drop button and introduced the sample cup to reach instantly the indicated pyrolysis temperature; the run was then immediately started.

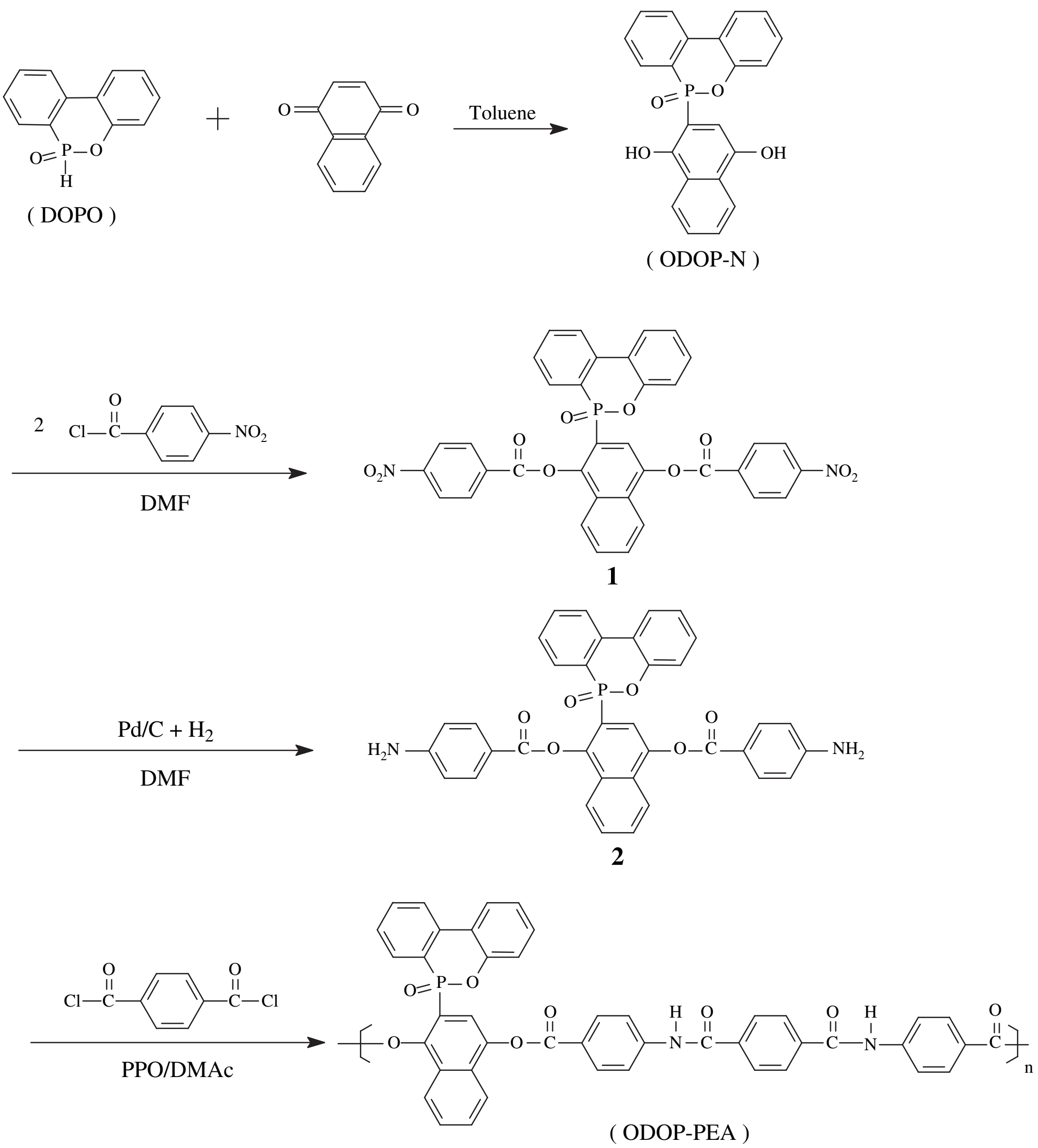

Scheme 1. Synthesis of ODOP-PEA.

Once the system started to run, the sample controller stopped sampling after 0.5 min and the pyrolysis gases from the ODOP-PEA sample were introduced directly into GC/MS analysis system. The operations were repeated at 350, 400, 450, 500, 550, 600, and 700 °C. Every procedure was repeated three times to ensure reproducibility. Pyrolysis-GC/MS analysis of the ODOP-N was also run by an analogous procedure and the pyrolysis temperatures were set at 275–600 °C.

The interface temperature of pyrolysis-GC/MS was set at 320 °C. The GC column is a F-Lab UA5-30M-0.25F metal capillary column (30 m × 0.25 mm i.d. with a coated film thickness of 0.25 μm) which shows higher thermal resistance up to 380 °C and is more effective in analyses of pyrolysates. The flow of the helium carrier gas was 1.0 mL/min. The GC oven temperature was initially held at 40 °C for 2 min, and then was programmed to 300 °C at 20 °C/min and held for 5 min. Total time of a sample run was 20 min. The GC inlet temperature was 320 °C, pressure 7.1 psi, total flow 14.1 mL/min, split ratio 10/1, and split flow 10 mL/min. The temperature of the GC/MS interface was set at 280 °C. The MS detector was scanned from 29 to 550 $m/z$ at a scan rate of 4.4 scans/s. Data analyses were searched by computer to match the database of Wiley275.L Mass Spectra Library.

The pyrolyser can also be operated in Evolved Gas Analysis-Mass Spectrometry (EGA-MS) mode to provide total ions as well as individual ions emission abundance versus temperature or time. The EGA-MS curves were generated by detecting evolved gases obtained by continuously heating a sample at a heating rate of 20 °C/min from 50 to 700 °C and at 700 °C the sample was held for 10 min. Thus, the EGA-MS mode started to run, the sample controller was continuously sampling for 42.5 min. The evolved gases for EGA-MS mode were introduced directly into GC/MS analysis system through an F-Lab UADTM-2.5M deactivated metal capillary column (2.5 m × 0.15 mm i.d. with a coated film thickness < 0.01 μm). The GC column was only 2.5 m and coated film thickness < 0.01 μm so that the evolved gases for EGA-MS mode were detected without any chromatographic separation. The GC oven temperature was held at 300 °C for 42.5 min. Total time of a sample run was 42.5 min.

## 3. Results and discussion

To prevent interference of polymer main chain decomposition, 2-(6-oxido-6*H*-dibenz[*c*,*e*][1,2]oxa-phosphorin-6-yl)-1,4-naphthalenediol (ODOP-N) was used as a model compound to elucidate the sequence of bond cleavage occurred within the pendant phosphorus-containing group. Thermal degradation mechanisms of the ODOP-N and ODOP-PEA are separately discussed below.

### 3.1. Pyrolysis of ODOP-N

As shown in Fig. 1, the EGA-MS curve of total ions of the ODOP-N displayed two overlapping peaks with maxima at around 320 and 470 °C, and a shoulder at around 550 °C. From the EGA-MS data, the pyrolysis temperatures of ODOP-N in pyrolysis-GC/MS were set at 275, 300, 350, 400, 450, 500, 550, and 600 °C, respectively. The total ion chromatograms (TIC) spectra of ODOP-N at flash pyrolysis temperatures between 275 and 600 °C are shown in Fig. 2. The pyrolysates at 600 °C were found to be biphenyl, 1,4-naphthoquinone, 1,4-naphthalenediol, 1-naphthol, 2-phenylphenol and dibenzofuran, respectively, with the increasing retention time in the pyrogram. The identified products listed in Table 1 accounted for about 95% of the pyrogram. The 1,4-naphthoquinone was the only product detected at 275 °C. The abundance of 1,4-naphthalenediol, 1-naphthol, dibenzofuran, and 2-phenylphenol increased as the temperature range increased from 300 to 450 °C. Biphenyl compound was observed at 500 °C. The pyrolysis mechanism of ODOP-N was proposed in Scheme 2.

The ODOP-N was first dissociated to give the DOPO and 1,4-naphthalenediol at 275 °C; then almost all the resulting 1,4-naphthalenediol were further thermally oxidized to yield 1,4-naphthoquinone at this temperature; however, at the condition of high concentration of 1,4-naphthalenediol due to the elevation of the pyrolytic temperature, some non-oxidized 1,4-naphthalenediol

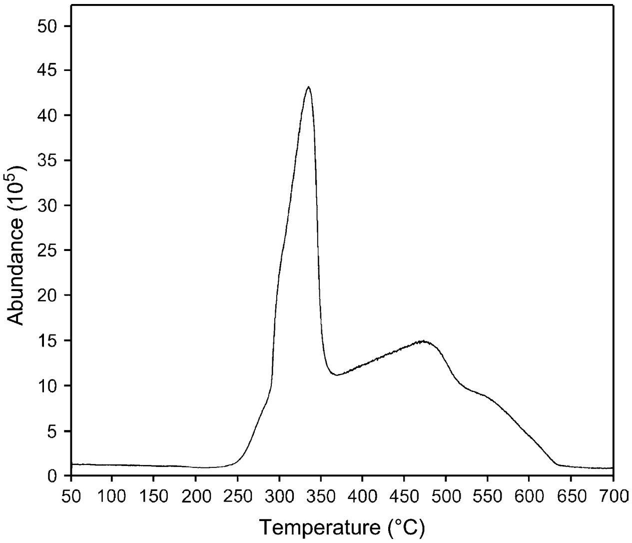

Fig. 1. The EGA-MS curve of total ions of the ODOP-N from 50 to 700 °C at a heating rate of 20 °C/min.

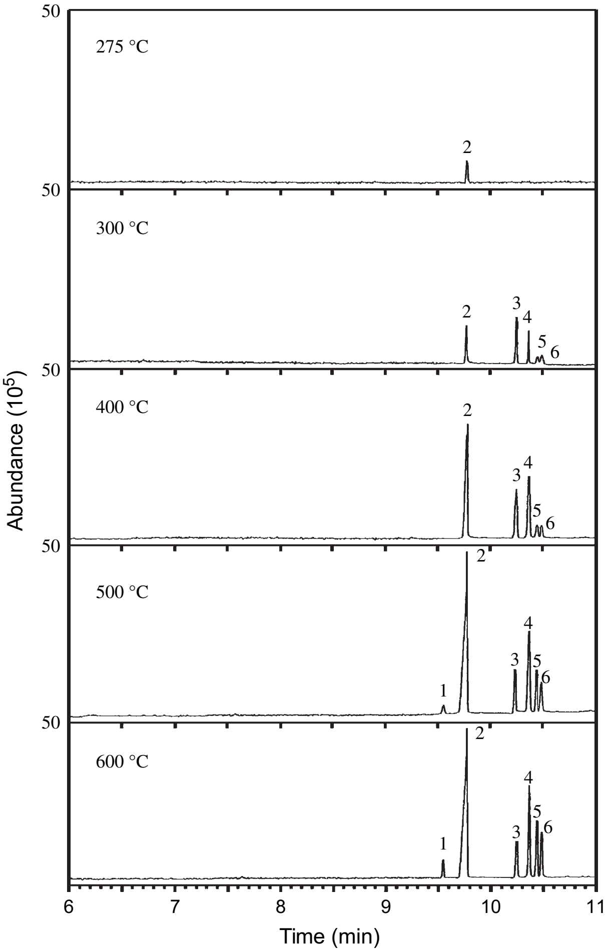

Fig. 2. The chromatograms of the pyrolysates of the ODOP-N at 275, 300, 400, 500, and 600 °C.

Table 1
Identification of the pyrolysates in pyrolysis-GC/MS of the ODOP-N at 600 °C

| Peak code | Structure | Compound | Retention time (min) | Molecular weight |
|---|---|---|---|---|
| 1 | 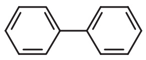 | Biphenyl | 9.55 | 154 |
| 2 | 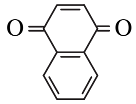 | 1,4-Naphthoquinone | 9.78 | 158 |
| 3 | 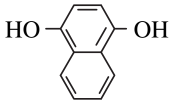 | 1,4-Naphthalenediol | 10.24 | 118 |
| 4 | 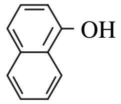 | 1-Naphthol | 10.37 | 160 |
| 5 | 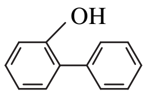 | 2-Phenylphenol | 10.44 | 170 |
| 6 | 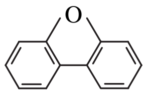 | Dibenzofuran | 10.49 | 168 |

still could be detected. The 1,4-naphthoquinone was stable and inert under the same pyrolytic condition. As the temperature was raised to higher than 300 °C, some of 1,4-naphthalenediol was further converted to 1-naphthol by the cleavage of the $C_{\text{naphthyl}}$–O bond. Due to its low volatility, the DOPO did not appear in the pyrogram and was further degraded to a diradical intermediate at 300 °C. The diradical intermediate was immediately cyclised to dibenzofuran or abstracted protons to form 2-phenylphenol. At 500 °C, biphenyl was evolved from the DOPO by the scission of P–$C_{\text{phenyl}}$ and O–$C_{\text{phenyl}}$ bonds.

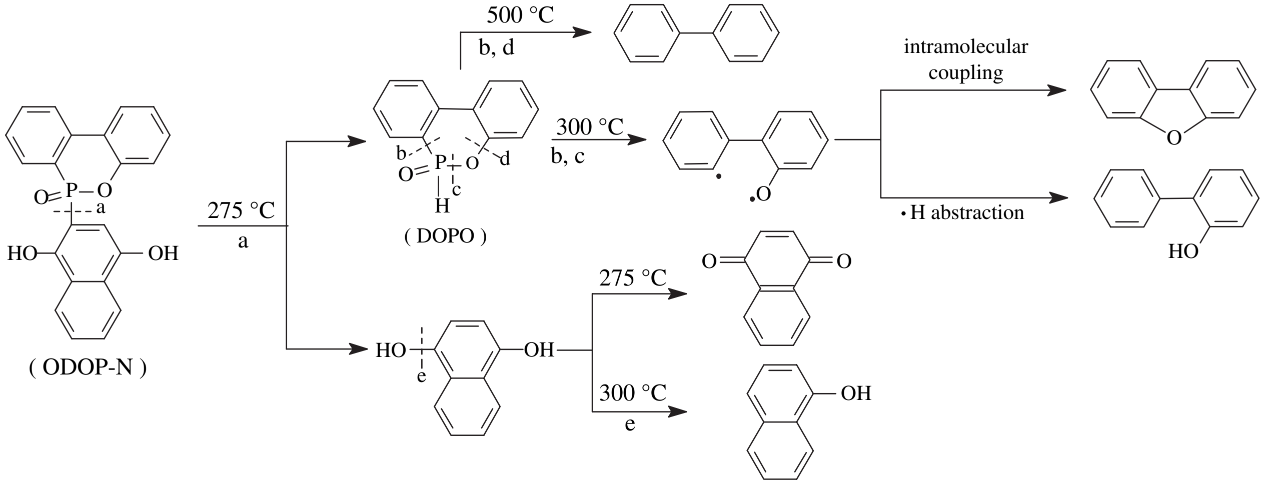

Scheme 2. The pyrolysis mechanism of the ODOP-N.

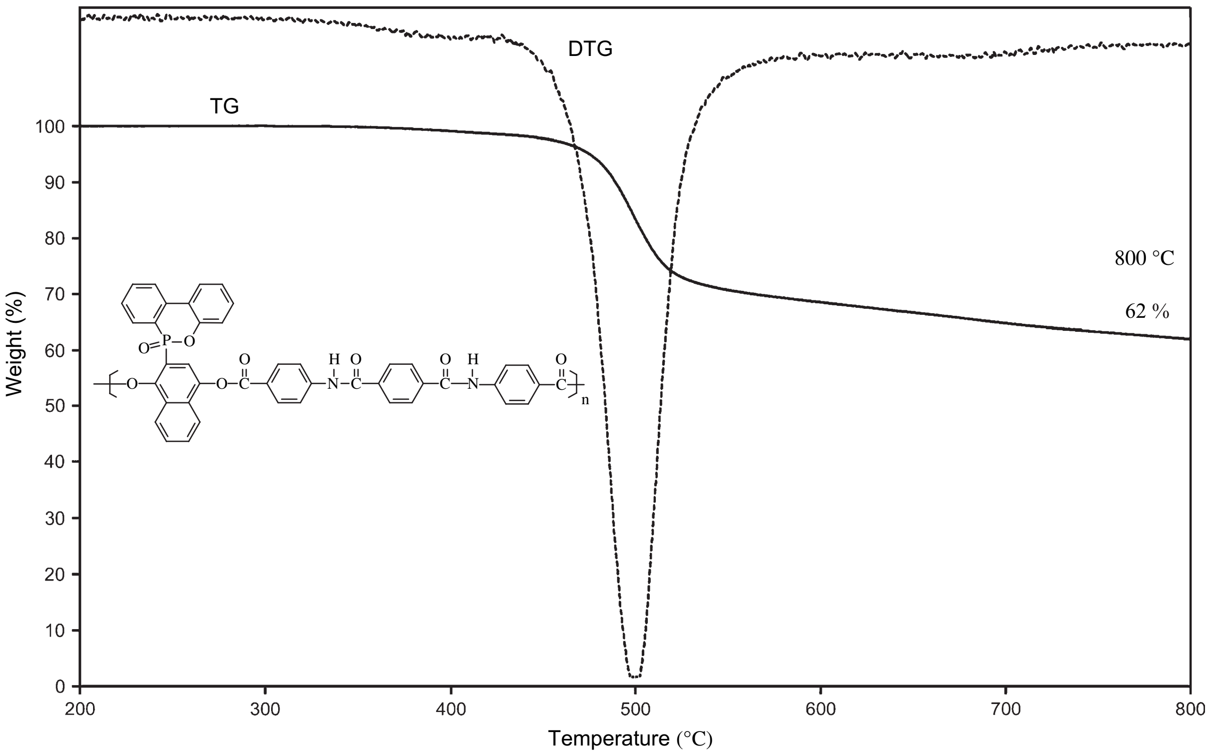

Fig. 3. The TG and DTG curves of the ODOP-PEA (heating rate = 20 °C/min).

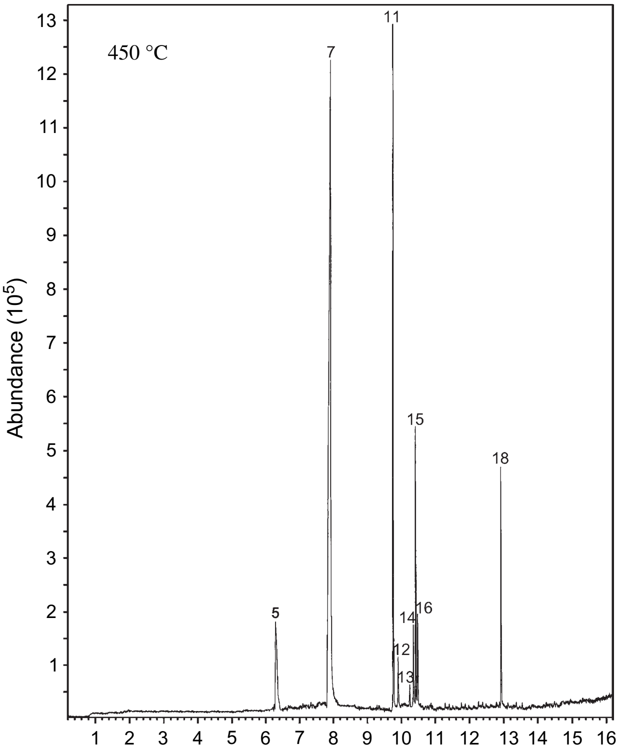

Fig. 4. The chromatogram of the pyrolysates of the ODOP-PEA at 450 °C.

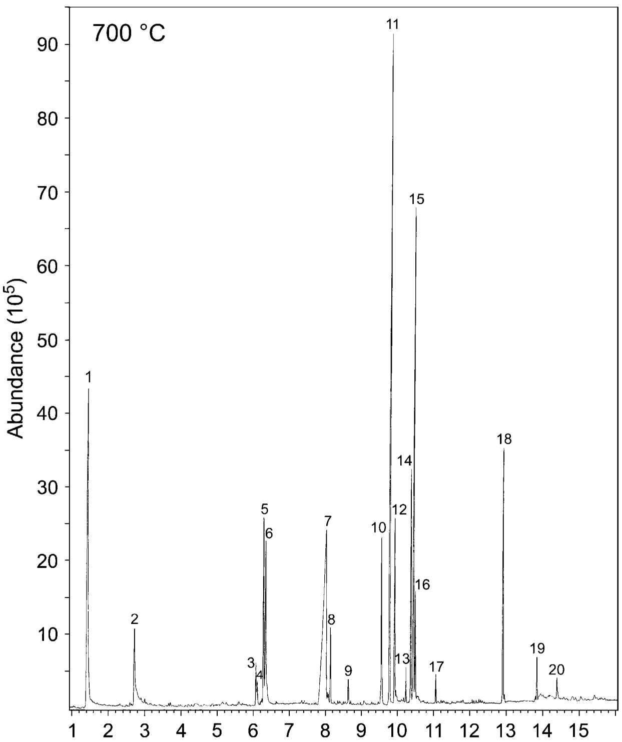

Fig. 5. The chromatogram of the pyrolysates of the ODOP-PEA at 700 °C.

Table 2
Identification of the pyrolysates in pyrolysis-GC/MS of the ODOP-PEA at 700 °C

| Peak code | Structure | Compound | Retention time (min) | Molecular weight |
|---|---|---|---|---|
| 1 | $CO_2$ | Carbon dioxide | 1.42 | 44 |
| 2 |  | Benzene | 2.72 | 78 |
| 3 | 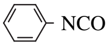 | Phenylisocyanate | 6.08 | 119 |
| 4 | 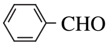 | Benzaldehyde | 6.11 | 106 |
| 5 | 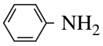 | Aniline | 6.28 | 93 |
| 6 | 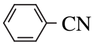 | Benzonitrile | 6.37 | 103 |
| 7 |  | Benzoic acid | 7.98 | 122 |
| 8 | 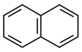 | Naphthalene | 8.15 | 128 |
| 9 | 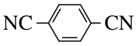 | Terephthalonitrile | 8.64 | 128 |
| 10 | 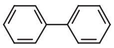 | Biphenyl | 9.55 | 154 |
| 11 | 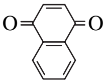 | 1,4-Naphthoquinone | 9.78 | 158 |
| 12 | 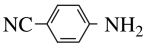 | 4-Aminobenzonitrile | 9.92 | 118 |
| 13 | 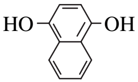 | 1,4-Naphthalenediol | 10.24 | 160 |
| 14 | 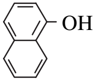 | 1-Naphthol | 10.37 | 144 |
| 15 | 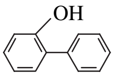 | 2-Phenylphenol | 10.44 | 170 |
| 16 | 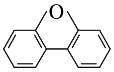 | Dibenzofuran | 10.49 | 168 |
| 17 | 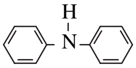 | Diphenylamine | 11.06 | 169 |
| 18 | 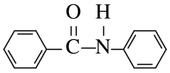 | Benzanilide | 12.93 | 197 |
| 19 | 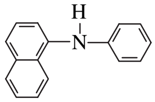 | *N*-Phenyl-1-naphthylamine | 13.85 | 219 |
| 20 | 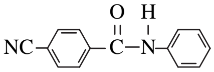 | 4-Cyanobenzanilide | 14.40 | 222 |

### 3.2. Pyrolysis of ODOP-PEA

The thermal stability of ODOP-PEA was characterized by TGA measurement in nitrogen atmosphere. As the TG and DTG curves shown in Fig. 3, the ODOP-PEA exhibited good thermal stability with insignificant weight loss up to 450 °C, although it began to decompose at about 300 °C. The ODOP-PEA decomposition reached the maximum at 500 °C, and at 800 °C there was 62% of charred residue left. To further investigate the thermal degradation mechanisms of the ODOP-PEA, pyrolysis-GC/MS was used with the pyrolysis temperatures set from 300 to 700 °C. Two typical chromatograms of the pyrolysates of the ODOP-PEA at 450 and 700 °C are shown in Figs. 4 and 5, respectively.

The pyrolysates were identified by mass spectra and are listed with increasing retention time in Table 2. Three major groups of pyrolysates are summarized in Table 2. The first group was 2-phenylphenol, dibenzofuran, and biphenyl originating from the bond scission in the pendant phosphorus group on the naphthalene ring. The second group was benzene, aniline, benzonitrile, benzoic acid, naphthalene, 1,4-naphthoquinone, 1,4-naphthalenediol, 4-aminobenzonitrile, 1-naphthol, benzanilide, phenylisocyanate, and terephthalonitrile which reflected the characteristic structure of the polymer backbone. The third group was the secondary reaction products such as diphenylamine and *N*-phenyl-1-naphthylamine.

In order to characterize the initial pyrolysis reactions of the ODOP-PEA, the temperature dependence of product formation was studied, and the results are summarized in Table 3. The dibenzofuran was the initial degradation product of the ODOP-PEA at 300 °C as shown in Table 3. At 350 °C, 2-phenylphenol was evolved together with dibenzofuran and its peak intensity increased appreciably between 400 and 500 °C. The 1,4-naphthoquinone, 1,4-naphthalenediol, and 1-naphthol were detected at 400 °C. The abundance of 1,4-naphthoquinone and 1-naphthol increased rapidly with temperature increase from 450 to 700 °C. Benzoic acid, benzanilide, 4-aminobenzonitrile, and aniline were detected at 450 °C. The peak intensity of aniline or 4-aminobenzonitrile was small, compared with that of benzanilide or benzoic acid, but they increased significantly in the temperature range of 550–700 °C. Biphenyl, phenylisocyanate, benzonitrile, 4-cyanobenzanilide, carbon dioxide, benzaldehyde, benzene as well as secondary species such as diphenylamine occurred at 500 °C. Terephthalonitrile, naphthalene, and secondary product such as *N*-phenyl-1-naphthylamine were observed at 550 °C.

Table 3
Detection temperatures of the pyrolysates of the ODOP-PEA

| Temperature (°C) | Pyrolysates |
|---|---|
| 300 | Dibenzofuran |
| 350 | 2-Phenylphenol |
| 400 | 1,4-Naphthalenediol, 1,4-naphthoquinone, 1-naphthol |
| 450 | Benzoic acid, benzanilide, aniline, 4-aminobenzonitrile |
| 500 | Biphenyl, phenylisocyanate, benzonitrile, 4-cyanobenzanilide<br>Benzene, diphenylamine, benzaldehyde, $CO_2$ |
| 550 | Terephthalonitrile, *N*-phenyl-1-naphthylamine, naphthalene |

On the basis of these results, the proposed pyrolysis mechanisms of ODOP-PEA are presented in Scheme 3. The release of dibenzofuran at 300 °C and 2-phenylphenol at 350 °C indicated that the initial degradation reactions occurred mainly at the pendant groups. As shown in Scheme 3(a), homolytic cleavages of the P–O and P–C bonds in the pendant group provided the diradical intermediate which could in turn undergo intramolecular coupling to dibenzofuran or abstract hydrogen from polymer chain to give 2-phenylphenol. The ratio of 2-phenylphenol to dibenzofuran was found to increase with the increased of the pyrolytic temperature. These results are consistent with the previous literature studies that the initial radicals formed at low temperatures would rapidly recombine to form a stable compound; whereas, the radicals formed at higher temperature would scavenge available hydrogen from the polymer chain.

Cleavage of ester linkage on the main backbone at 400 °C gave 1,4-naphthalenediol, 1,4-naphthoquinone, and 1-naphthol. The hydrolysis of the ester linkage by the adsorbed water gave 1,4-naphthalenediol, and most of it was further thermally oxidized to yield 1,4-naphthoquinone, especially at higher pyrolysis temperature. The formation of 1-naphthol represented the assumption that homolytic scission of the $C_{naphthyl}$–O bond also occurred at 400 °C.

Benzanilide, benzoic acid, aniline, and 4-aminobenzonitrile were detected at 450 °C, and this provided the clue for the amide linkage disconnection at this temperature. The presence of benzanilide could be accounted by homolytic cleavage of the $C_{phenyl}$–$C_{carbonyl}$ bonds at the amide linkage (labeled as h and j in Scheme 3(a)) with subsequent protonation. The formation of 4-aminobenzonitrile was resulted from initial $C_{phenyl}$–N cleavage (labeled as g and i in Scheme 3(a)) followed by a Hofmann type rearrangement to form an isocyanate which hydrolyzed to yield the amine moiety. Benzoic acid was mainly released from ester hydrolysis of the main chain followed by the homolytic scission of the $C_{phenyl}$–N bond (labeled as f and g in Scheme 3(a)). The abundance of aniline formation was small at temperature < 500 °C as compared with the abundance of benzoic acid formation, but it increased sharply at temperature ≧ 500 °C. From this result, we assumed that aniline formed at low temperature was

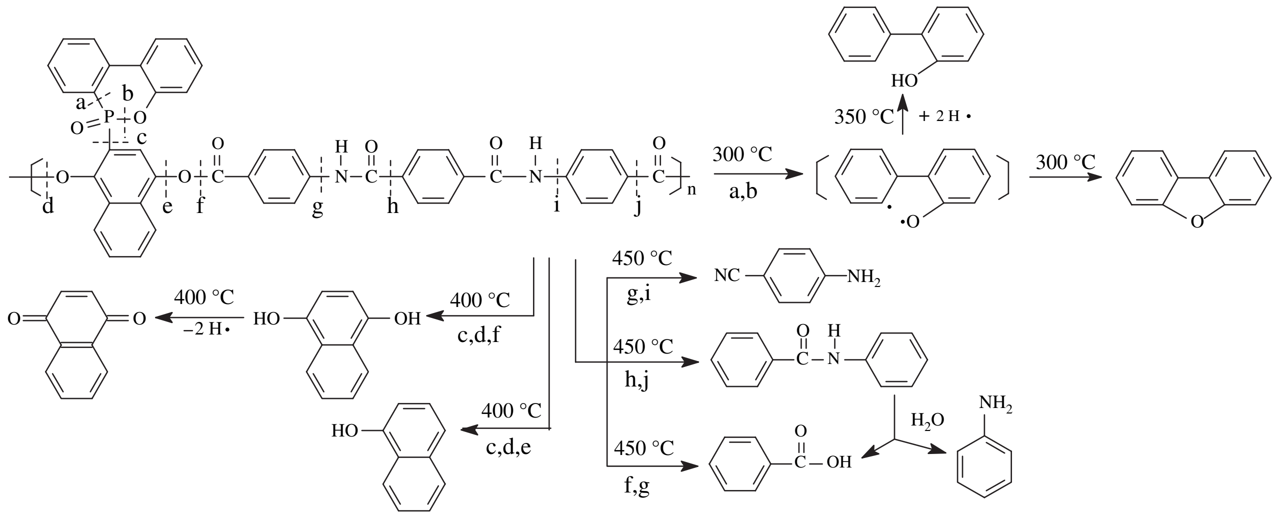

(a) 300-450 °C

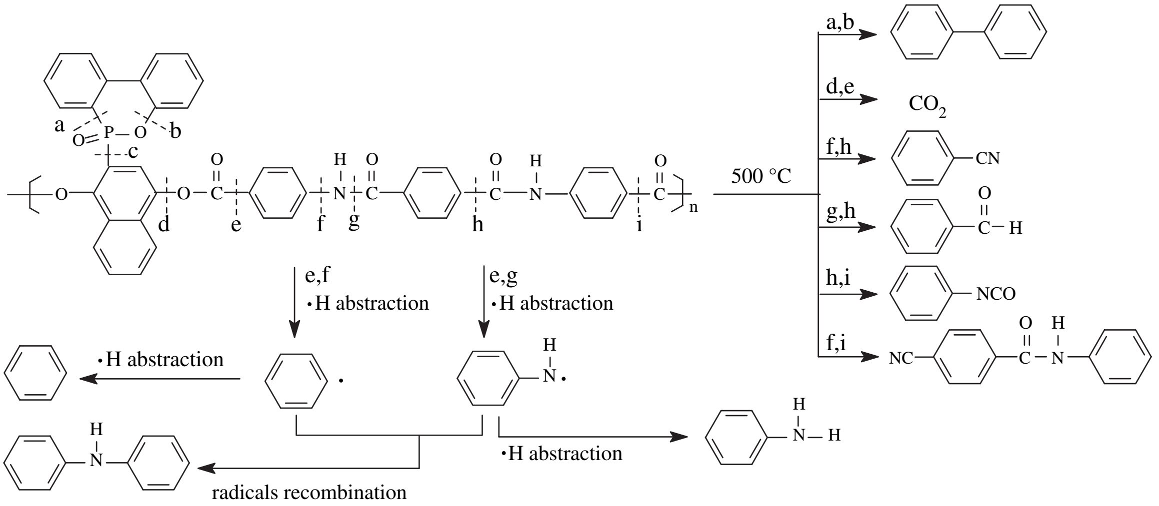

(b) 500 °C

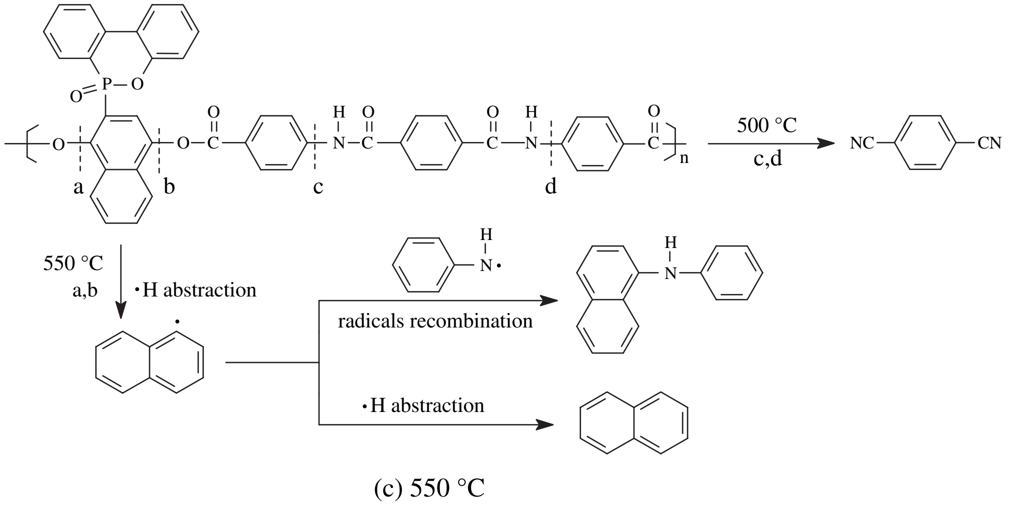

(c) 550 °C

Scheme 3. The pyrolysis mechanisms of the ODOP-PEA at (a) 300–450 °C; (b) 500 °C and (c) 550 °C.

a secondary product from hydrolysis of amide bond in benzanilide, whereas the formation of aniline at higher temperature (≧500 °C) should be the homolytic cleavage of $C_{carbonyl}$–N bond of the amide linkage.

At 500 °C, the benzaldehyde was one of the pyrolysates, and the occurrence of benzaldehyde was a direct evidence to support the above statement that homolytic cleavage of amide bond occurred at this temperature. The evolution of phenylisocyanate, at 500 °C, occurred from the homolytic cleavage of the $C_{phenyl}$–$C_{carbonyl}$ bond followed by hydrogen radical elimination. The nitrile functionality of benzonitrile and 4-cyanobenzanilide was considered to form through homolytic cleavage of the $C_{phenyl}$–N bond followed by protonation and dehydration. Thermal decarboxylation of benzoic acid also occurred at 500 °C to release carbon dioxide and benzene. As shown in Scheme 3(b), phenyl radical and aniline radical formed by homolytic bond scission might either abstract a proton to give benzene and aniline, respectively, or combine each other to give diphenylamine.

At 550 °C, the evolution of terephthalonitrile might be explained by homolytic cleavage of the $C_{phenyl}$–N bond followed by protonation and dehydration. As shown in Scheme 3(c), 1-naphthyl radical formed by homolytic bond scission of $C_{naphthyl}$–O bond might either abstract a proton to give naphthalene or associate with aniline radical to give *N*-phenyl-1-naphthylamine.

In our preliminary investigation on the thermal decomposition of a representative poly(ester-amide) (PEA) indicated that the breakage of the ester linkages started at 350 °C, which initiated the polymer chain scission. The subsequent degradation of the PEA involved in the bond cleavage of the amide linkages and the secondary reaction of pyrolysis products at elevated temperatures [16]. This result is also in good agreement with the main chain degradation behaviour of the ODOP-PEA, indicating that the pendant phosphorus-containing groups had no significant effect on polymer main chain decomposition but the initial thermal degradation temperature of polymer main chain was elevated to 400 °C.

## 4. Conclusion

The thermal degradation behaviour of the novel phosphorus-containing aromatic poly(ester-amide) (ODOP-PEA) compound was identified in this study. The TG and DTG curves of the ODOP-PEA showed a slight weight loss at the temperature range of 300–400 °C followed by a main decomposition at 500 °C. Results from pyrolysis-GC/MS suggested that the slight weight loss at the temperature range of 300–400 °C resulted from bond cleavage of the pendant phosphorus groups. A major weight loss peak with a maximum decomposition temperature at 500 °C was attributed to the main chain scission. In conclusion, thermal degradation mechanism of the poly(ester-amide) main chain is not altered by the incorporation of bulky phosphorus-containing groups into polymer as pendant groups. P–C bond linked between the pendant group and the polymer main chain is the weakest bond in the ODOP-PEA and degrades at 275 °C. P–O bond in pendant phosphorus-containing group is stable up 300 °C as verified by pyrolysis-GC/MS analysis.

## Acknowledgements

The authors are grateful to the National Science Council of the Republic of China for the financial support of this work.

## References

[1] Cassidy PE. Thermally stable polymers. New York: Marcel Dekker; 1980.
[2] Yang HH. Aromatic high-strength fibers. New York: John Wiley & Sons; 1989.
[3] Yang HH. Kevlar aramid fiber. New York: John Wiley & Sons; 1993.
[4] Maglio G, Palumbo R, Vignola MC. Macromol Chem Phys 1995;196:2775.
[5] Hsiao S-H, Yu C-H. J Polym Res 1996;3:247.
[6] Hsiao S-H, Huang P-C. Macromol Chem Phys 1997;198:4001.
[7] Hsiao S-H, Yang C-P, Chen S-H. Polymer 2000;41:6537.
[8] Espeso JF, de la Campa JG, Lozano AE, de Abajo J. J Polym Sci A Polym Chem 2000;38:1014.
[9] Espeso JF, Ferrero E, de la Campa JG, Lozano AE, de Abajo J. J Polym Sci A Polym Chem 2001;39:475.
[10] Liaw D-J, Liaw B-Y, Yang C-M. Macromol Chem Phys 2001;201:1866.
[11] Liou G-S, Hsiao S-H. J Polym Sci A Polym Chem 2002;40:1781.
[12] Imai Y. High Perform Polym 1995;7:337.
[13] Imai Y. React Funct Polym 1996;30:3.
[14] Liaw D-J, Liaw B-Y, Jeng M-Q. Polymer 1998;39:1597.
[15] Wu S-C, Shu C-F. J Polym Sci A Polym Chem 2003;41:1160.
[16] Hsiao S-H, Leu W-T, Guo W. Polym J 2002;34:925.
[17] Wang C-S, Lin C-H. J Polym Sci A Polym Chem 1998;36:3051.
[18] Wang C-S, Shieh J-Y. Polymer 1998;39:5819.
[19] Wang C-S, Lin C-H. Polymer 1999;40:747.
[20] Wang C-S, Lin C-H. J Polym Sci A Polym Chem 1999;37:891.
[21] Wang C-S, Lin C-H. Polymer 1999;40:4387.
[22] Wang C-S, Lin C-H. Polymer 1999;40:5665.
[23] Wang C-S, Lin C-H. J Polym Sci A Polym Chem 1999;37:3903.
[24] Wang C-S, Shieh J-Y. J Appl Polym Sci 1999;73:353.
[25] Wang C-S, Lee M-C. Polymer 2000;41:3631.
[26] Liou G-S, Hsiao S-H. J Polym Sci A Polym Chem 2002;40:459.
[27] Liu Y-L, Tsai S-H. Polymer 2002;43:5757.
[28] Liau C-K, Yang C-K, Viswanath S. Polym Eng Sci 1996;36:2589.
[29] Hornsby PR, Wang J, Rothon R, Jackson G, Wilkinson G, Cossick K. Polym Degrad Stab 1996;51:235.
[30] So Y-H, Froelicher SW, Kaliszewski B, DeCaire R. Macromolecules 1999;32:6565.
[31] Perng L-H. J Polym Res 2000;7:185.
[32] Perng L-H. J Appl Polym Sci 2001;79:1151.
[33] Endo K, Yamashita S, Ishibashi Y, Nishikawa K. (Sanko Chemical Co.). Jpn. Kokai Tokkyo Koho 5–331179; 1993.
[34] Liou G-S, Hsiao S-H. J Polym Sci A Polym Chem 2001;39:1786.